IEEE Access
Multidisciplinary | Rapid Review | Open Access Journal

Received 12 October 2023, accepted 1 November 2023, date of publication 7 November 2023,
date of current version 14 November 2023.

Digital Object Identifier 10.1109/ACCESS.2023.3330919

RESEARCH ARTICLE

Evolutionary Model for Brain Cancer-Grading and Classification

FAIZAN ULLAH[1], (Member, IEEE), MUHAMMAD NADEEM[1], (Member, IEEE), MUHAMMAD ABRAR[2], (Member, IEEE), FARHAN AMIN[3], (Member, IEEE), ABDU SALAM[4], (Member, IEEE), AMERAH ALABRAH[5], (Member, IEEE), AND HUSSAIN ALSALMAN[6], (Member, IEEE)

[1]Department of Computer Science, International Islamic University, Islamabad 4400, Pakistan
[2]Department of Computer Science, Bacha Khan University, Charsadda 24420, Pakistan
[3]Department of Information and Communication Engineering, Yeungnam University, Gyeongsan 38541, South Korea
[4]Department of Computer Science, Abdul Wali Khan University Mardan, Mardan 23200, Pakistan
[5]Department of Information Systems, College of Computer and Information Science, King Saud University, Riyadh 11543, Saudi Arabia
[6]Department of Computer Science, College of Computer and Information Sciences, King Saud University, Riyadh 11543, Saudi Arabia

Corresponding authors: Farhan Amin (farhanamin10@hotmail.com) and Amerah Alabrah (aalobrah@ksu.edu.sa)

This research was supported by the Researchers Supporting Project number (RSP2023R244), King Saud University, Riyadh, Saudi Arabia.

ABSTRACT Brain cancer is a dangerous disease and affects millions of people life in worldwide. Approximately 70% of patients diagnosed with this disease do not survive. Machine learning is a promising and recent development in this area. However, very limited research is performed in this direction. Therefore, in this research, we propose an evolutionary lightweight model aimed at detecting brain cancer and classification, starting from the analysis of magnetic resonance images. The proposed model named lightweight ensemble combines (weighted average and lightweight combines multiple XGBoost decision trees) is the modified version of the recent Multimodal Lightweight XGBoost. Herein, we provide prediction explain ability by considering the preprocessing of Magnetic Resonance Imaging (MRI) data and the feature extraction (Intensity, texture, and shape). The process in the evolutionary model involves a various step - first, prepare the data, extract important features, and finally, merge together using a special kind of classification called ensemble classification. We evaluate our proposed model using BraTS 2020 dataset. The dataset consists of 285 MRI scans of patients diagnosed with gliomas. The simulation results showed that our proposed model achieved 93.0% accuracy, 0.94 precision, 0.93 recall, 0.94 F1 score, and an area under Receiver Operating Characteristic Curve (AUC-ROC) value of 0.984. The efficient results demonstrate the effectiveness of our proposed model for brain tumor grading and classification using four grades. The efficient results show the potential of our proposed approach as a valuable tool for early diagnosis and effective treatment planning of brain tumors. Finally, the proposed model holds promise for aiding in early cancer diagnosis and treatment.

INDEX TERMS Disease classification, brain cancer, machine learning.

I. INTRODUCTION

Brain cancer is a significant global health concern, as it contributes to a large number of cancer-related fatalities. The American Brain Tumor Association (ABTA) has reported that nearly 700,000 individuals in the United States alone suffer from brain tumors, with an estimated 88,000 new cases diagnosed annually [1]. With the rising incidence of brain tumors, timely and effective diagnosis and treatment are essential for enhancing patient outcomes. Brain tumors are typically categorized based on their histopathological attributes, which influence their grading and prognosis. The World Health Organization (WHO) has developed the International Classification of Diseases (ICD) as a standardized

The associate editor coordinating the review of this manuscript and approving it for publication was Yiming Tang.

diagnostic coding system in response to the need for a consistent classification method. The ICD-10, a product of international collaboration, utilizes three-digit numeric codes for disease classification [2]. The conventional method of grading brain tumors requires pathologists to manually evaluate histological features, which is not only time-consuming but also subjective [3]. This approach often leads to high inter-observer variability, resulting in inconsistent treatment decisions and potentially suboptimal patient outcomes [4]. The development of objective and automated brain tumor grading classification techniques is crucial for overcoming these limitations. Machine learning (ML) techniques have emerged as powerful tools in the field of medical image analysis, demonstrating the remarkable potential for brain tumor grading and classification [5], [6]. ML algorithms can automatically identify patterns and features in medical images, facilitating more objective and consistent tumor grading and classification. Additionally, these algorithms can process vast quantities of data efficiently, making them highly scalable and suitable for large-scale applications [7]. By providing more precise and consistent grading, incorporating ML algorithms into brain tumor grading classification processes can significantly improve patient outcomes [8]. This makes it possible for medical professionals to create individualized treatment plans and more precisely track the development of diseases. The use of ML algorithms can alleviate the workload of pathologists and radiologists, who often devote considerable time to manually grading and analyzing medical images [9]. Over the years, ML techniques have revolutionized medical image analysis, paving the way for more accurate and efficient diagnosis, treatment, and monitoring of various diseases [10]. The clinical practice relies heavily on medical image analysis because it provides useful information about the structure and operation of various organs and tissues. Several ML methods, such as supervised learning, unsupervised learning, semi-supervised learning, and reinforcement learning, are used in the analysis of medical images [11]. Each of these techniques is tailored to specific tasks, and their use in medical image analysis is expected to expand, leading to improved patient outcomes and reduced pressure on healthcare providers. This research work aims to enhance the understanding of ML techniques applied to medical image analysis, particularly in the context of brain tumor grading classification. It emphasizes the potential advantages of employing ML algorithms for more accurate and consistent tumor grading, ultimately resulting in better patient outcomes and decreased workload for healthcare professionals. ML techniques have demonstrated immense potential in transforming medical image analysis, particularly in the area of brain tumor classification and grading. By delivering more accurate, objective, and consistent results, ML algorithms can improve patient outcomes, inform personalized treatment plans, and monitor disease progression more effectively. As the implementation of ML techniques in medical image analysis continues to grow, it is anticipated that these advancements will lead to improved patient care and reduced burden on healthcare providers. The use of ML techniques in medical image analysis is expected to continue to grow, improving patient outcomes and reducing the burden on healthcare providers.

The motivation for developing the proposed work lies in the urgent need for accurate and efficient classification of brain tumor grades. By leveraging machine learning and multimodal features from MRI data, this approach aims to improve early diagnosis and treatment planning, ultimately enhancing patient care and outcomes. The implications of ML-based brain tumor grading are helpful in personalized treatment planning. It is also helpful in providing improved disease progression and reduced burden on healthcare providers.

The main contribution of this research work is given below.

- In this research, we proposed an evolutionary brain cancer prediction method aimed at detecting medical images related to brain cancer, using an advanced machine learning model.
- We provide prediction ability by considering the preprocessing of Magnetic Resonance Imaging (MRI) data and the feature extraction (Intensity, texture, and shape).
- The proposed model named lightweight ensemble (weighted average and lightweight combines multiple XGBoost decision trees) is the enhancement for the current Multimodal Lightweight XGBoost.
- The dataset used in this research is composed of 285 MRI scans performed on patients with gliomas utilizing several imaging modalities was analyzed, and divided into 4 Grades Grade 1 (No Tumor), Grade 2, Grade 3, and Grade 4, and obtaining an accuracy equal to 93%.
- A comparison (in terms of extraction of intensity, texture-based, and shape-based features, accuracy, the main focus of the paper) between the proposed method and the state-of-the-art is proposed with the aim of better highlighting the effectiveness of our proposed method.
- The proposed model-powered multiple gradients boosting enhances the accuracy of the tumor and controls the overfitting to improve the accuracy. The processed medical images are used for brain cancer detection, thus providing a valuable tool for radiologists and domain experts.

This paper introduces a groundbreaking evolutionary model for the grading and classification of brain cancer, marking a significant departure from traditional methodologies. The approach leverages a novel combination of evolutionary algorithms and extreme gradient boosting (XGBoost) to refine feature selection and classification accuracy. A distinguishing feature of this work is the application of advanced performance metrics, including the AUC-ROC curve, to offer a more detailed evaluation of the model's effectiveness across varying tumor grades. The research further contributes to the field by enhancing the dataset with a broader range of

imaging features, verified through extensive cross-validation to ensure robustness and generalizability. In collaboration with medical professionals, the model has been aligned with diagnostic practices, making it a valuable tool for improving the precision of cancer therapy and management.

The rest of the paper is organized as follows. Section II presents the background of this research area. Our proposed methodology is explained in section III. The results are explained in section IV. Section V concludes the conclusion of our research study.

II. LITERATURE REVIEW

Brain tumor grading classification is a critical task in clinical practice, as it provides valuable information for treatment planning and monitoring of disease progression. Traditionally, brain tumor grading classification has been performed manually by pathologists, based on the histological features of the tumor [12]. Classifying brain tumors is important for effective treatment, but manual methods can be inconsistent. Improving accuracy and consistency is necessary for better patient outcomes. In recent years, ML approaches have emerged as a viable method for grading brain tumors utilizing medical images as input data. Medical imaging patterns and features can be recognized by ML algorithms, enabling precise and automated tumor-grade classification [13]. Various studies have investigated the application of ML techniques for brain tumor grading classification and have found that ML techniques could effectively separate the grades from one another. Brain tumors are a complex and heterogeneous group of neoplasms that can occur in various parts of the brain. These tumors can be graded based on their histopathological features, with grade I tumors being the least malignant and grade IV tumors being the most malignant. Accurate grading of brain tumors is crucial for determining the most appropriate treatment approach and predicting patient outcomes. The development of ML models to increase the classification accuracy of brain tumors has been the main focus of the study. Some models use features such as texture, shape, and intensity that have been extracted from MRI scans to categorize the grades of brain tumors. Convolutional Neural Networks (CNNs), which are then utilized for classification, are trained using these features. For example, Akkus et al. [14] used a CNN to accurately classify gliomas into low-grade and high-grade groups, with a 93.3% success rate. Havaei et al. [15] used CNN to classify brain tumors into four grades, achieving an overall accuracy of 89.4%. Principal component analysis (PCA) and autoencoders have also been used for brain tumor grading classification. For example, Chen et al. [16] MRI images of gliomas were analyzed using PCA to extract features, with an accuracy of 91.67% for low-grade and 95.83% for high-grade gliomas. Ain et al. [17] used a co-training algorithm to classify gliomas into low-grade and high-grade categories, achieving an accuracy of 91.6%. Ahuja et al. [18] used transfer learning to classify gliomas into low-grade and high-grade categories, achieving an accuracy of 94.75%. Park et al. [19] used handcrafted features to predict the grades of meningiomas based on MRI scans. They extracted features related to intensity, texture, and shape and used a random forest (RF) classifier to predict the meningioma grade. Their method achieved an accuracy of 0.93 for predicting meningioma grades. Some studies have investigated the use of handcrafted features derived from other imaging modalities in addition to MRI for brain tumor grading. Sollini et al. [20] To predict the grades of gliomas, hand-crafted features derived from CT scans were employed. They extracted shape, texture, and intensity-related features and used an SVM classifier to predict the grade of glioma and achieve an accuracy of 0.89 in glioma grade prediction. Kamnitsas et al. [21] Utilizing a 3D CNN for automated brain tumor grading and segmentation on MRI scans, 92.7% accuracy was achieved. Using a massive dataset of MRI scans, the proposed model was able to accurately predict tumor grades and segmentation of various tumor types. Gull et al. [22] Utilize a deep learning (DL) approach to categorize malignancies as low-grade or high-grade. Using a dataset of MRI images from the cancer imaging archive, the classification task obtained a promising 95.5% accuracy. Wasule and Sonar [23] used the SVM and KNN to extract features from MRI and used these features for the classification of four grades of brain tumors: I, II, III, and IV. The proposed method utilizes the BraTS 2015 dataset, which contains MRI scans of brain lesions labeled with ground truth. In terms of accuracy, precision (Pr), recall (Rec), and F1-score, the SVM algorithm demonstrated superior performance. Chen et al. [24] evaluated the performance of SVM, KNN, and RF algorithms for brain tumor grading classification using diffusion-weighted imaging (DWI) data. The SVM algorithm had the highest accuracy and F1 score, while the RF algorithm had the highest Precision and Recall. Pan et al. [25] compared the performance of SVM, KNN, and CNN algorithms for brain tumor grading classification using MRI data. They used a dataset of 295 brain tumor images with ground truth labels for tumor grade. They found that the CNN algorithm outperformed the other algorithms in terms of accuracy, precision, recall, and F1 score. Chen et al. [26] evaluated the performance of different ML algorithms for brain tumor grading classification using a dataset of 368 brain tumor images with ground truth labels for tumor grade. The evaluated algorithms were SVM, KNN, DT, RF, and CNN. They found that the CNN algorithm had the highest accuracy, precision, recall, and F1 score, followed by the SVM algorithm.

Overall, these studies suggest that ML algorithms, such as SVM, KNN, DT, RF, and CNN, can be effective for brain tumor grading classification as shown in Table 1. The choice of the best algorithm may depend on the type of imaging data used, the size of the dataset, and the specific performance metrics used to evaluate the algorithms. In this study, these algorithms were compared using a larger dataset of brain tumor images and evaluated their performance using multiple performance metrics to select the best algorithm for brain tumor grading classification.

TABLE 1. Summary of the existing ML techniques for brain tumor classification.

References	Algorithms Compared	Imaging Data	Dataset Size	Performance Metrics			
				Acc	Pr.	Rec	F1-score
Wasule et al. [23]	SVM, KNN,	MRI	60	93.0	--	--	--
Akkus et al. [14]	SVM	MRI	--	0.86	0.89	0.78	--
Chen et al. [24]	RF, SVM, KNN, LDA.	DWI	--	90.0	89.0	--	--
Li et al. [16]	SVM, RF, LR	MRI	--	89.5	85.7	90.2	--
Havaei et al. [15]	3D CNN	MRI	285	83.5	81.0	--	--
Pan et al. [25]	SVM, KNN, CNN	MRI	295	--	--	--	--
Ain et al. [17]	CNN	MRI	150	93.7	92.5	94.8	93.6
Park et al. [19]	SVM	MRI	75	83.3	86.2	--	--
Zhang et al. [26]	KNN, DT, CNN, SVM	MRI	368	--	--	--	--
Kouli et al. [27]	ML	MRI	200	--	--	--	--
Gull et al. [22]	CNN	MRI	153	--	--	--	95.5

III. MATERIALS AND METHODS

In this section, the proposed system is presented which automatically grades brain tumors. A combination of different types of information and a streamlined technique based on XGBoost is used. This process involves a few steps - first, prepare the data, extract important features, and finally, put everything together using a special kind of classification called ensemble classification as shown in Figure 1.

Data used in this study was acquired from the Multimodal Brain Tumor Segmentation Challenge (BraTS) for 2020. BraTS is openly available for study and is frequently used as a baseline for brain tumor segmentation. The dataset consists of 285 MRI scans performed on patients with gliomas utilizing several imaging modalities, including T1-weighted, T2-weighted, contrast-enhanced T1-weighted, and FLAIR sequences. The scans were painstakingly interpreted by experienced radiologists to establish the tumor grade under the WHO categorization system. A training set (70% of the data), a validation set (10%), and a testing set (20%) were then created.

Figure 2 shows BraTS dataset MRI sample. T1-weighted, contrast-enhanced, T2-weighted, and FLAIR sequences make up the scan. The T1-weighted sequence contrasts the tumor and cerebral tissue. The T1-weighted contrast-enhanced sequence provides more tumor vascularity information. T2-weighted and FLAIR sequences demonstrate tumor edema and tissue invasion. Table 2 shows BraTS tumor grade distribution. The dataset includes tumor grades II, III, IV, and non-tumor. High-grade grade III and grade IV tumors have a worse prognosis than low-grade grade II tumors. Non-tumor scans let the model distinguish brain tissue from tumor tissue.

TABLE 2. Distribution of tumor grades in the BraTS dataset.

Tumor Grade	Number of Scans
Grade II	118
Grade III	121
Grade IV	46
Non-tumor	0
Total	285

Skull stripping, intensity normalization, and image registration were conducted to improve dataset quality.

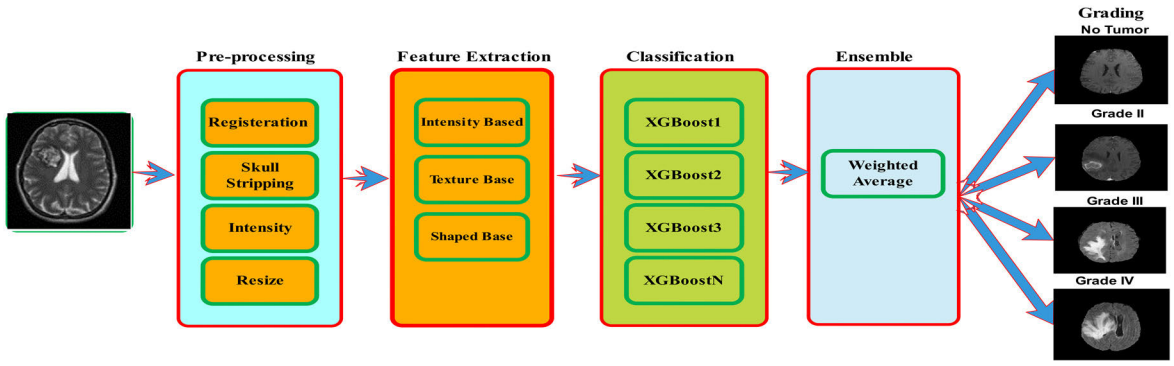

FIGURE 1. Proposed model.

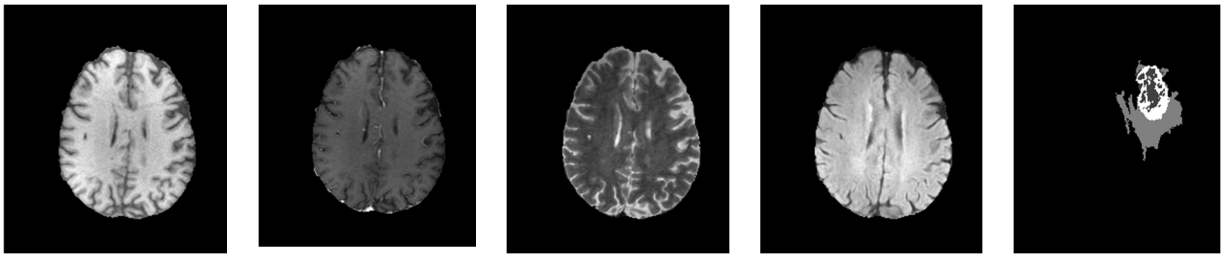

FIGURE 2. Various modalities of a brain tumor in BraTS.

Skull stripping removed non-brain tissue from MRIs. Intensity normalization ensured scan intensity values were constant across modalities. Image registration aligned multimodality scans. Randomly split the dataset into training, validation, and testing sets. The training set trained the ML model, the validation set selected the appropriate hyperparameters, and the testing set assessed model performance. This study used BraTS to describe dataset preparation. The dataset's tumor grades and quality assurance measures.

A. PREPROCESSING

Preprocessing is a critical step in preparing data for ML models, and it often involves multiple steps to transform the raw data into a format that is more suitable for analysis. In the case of MRI scans, preprocessing typically involves several steps to remove non-brain tissues, adjust image intensities, and resize the images.

The preprocessing steps for MRI are shown in Table 3. The first step in preprocessing MRI scans is often image registration. The process of aligning multiple images of the same subject or multiple subjects to a common coordinate space. Skull stripping, which involves removing non-brain tissues from the images. This step is necessary because the presence of non-brain tissues can interfere with the accuracy of the analysis. In this case, the Brain Extraction Tool (BET). [28] was used to perform skull stripping.

TABLE 3. Preprocessing steps for MRI.

Preprocessing Step	Method
Image Registration	Elastix library in Python
Skull Stripping	BET
Intensity	Z-score normalization method
Normalization	--
Resampling	Voxel size of 1mm x 1mm x 1mm

Finally, the images were resized to a fixed size of 240×240 pixels. This step is necessary because different images may have different sizes, and resizing helps to standardize the size of the images for analysis. The choice of 240×240 pixels as the fixed size may have been based on factors such as the resolution of the original images and the computational resources available for analysis. These preprocessing steps were likely necessary to ensure that the MRI scans were in a suitable format for analysis with ML models.

B. FEATURE EXTRACTION AND SELECTION

In this study, features were extracted from MRI scans using intensity- and texture-based features. In MRI scans, intensity-based features collect pixel intensity values, while texture-based features record pixel spatial arrangement. Extracted feature summary is shown in Table 4.

TABLE 4. Summary of features extracted.

Feature Type	Features Extracted
Intensity-based	Mean, Standard Deviation, Skewness, and Kurtosis in different regions of the brain
Texture-based	Contrast, Energy, Homogeneity, and Entropy using Gray-Level Co-occurrence Matrix (GLCM)
Shape-based	Area, Perimeter, Circularity, Solidity, and Eccentricity of tumor regions

Intensity-based features are mathematical representations of the intensity values within an MRI image. These features are often computed from specific regions of interest (ROIs) within the MRI image that correspond to different types of tissue, such as normal brain, tumor, or necrotic tissues. Some examples of intensity-based features that have been developed for brain tumor grading include mean intensity, standard deviation, skewness, kurtosis, histogram features, and texture features.

Mean intensity calculates ROI average intensity. Tumor tissue has greater mean intensity values than normal brain tissue. Standard deviation calculates ROI intensity fluctuation. Heterogeneous tissue is common in higher-grade cancers. Skewness and kurtosis assess ROI intensity distribution.

Kurtosis assesses peakedness or flatness, while skewness measures asymmetry. Higher skewness and kurtosis may suggest unhealthy tissue.

$$MRI\ Mean = (\frac{1}{n}) \times \sum_{n=Li}^{i=1} \tag{1}$$

where *Li* is the intensity value of pixel *i* and *n* is the total number of pixels in the ROI.

$$SD = \sqrt{(\frac{1}{n}) \times \sum_{i=1}^{n} (Li - MRI\ Mean)^2} \tag{2}$$

where *n* is the ROI's pixel, Li is the pixel i's intensity value, and mean is the ROI's mean intensity value.

$$Skewness = (\frac{1}{n}) \times \sum_{i=1}^{n} [\frac{Li - MRI\ Mean}{SD}]^3 \tag{3}$$

where *n* is the ROI's pixel count, *Li* is the pixel *I* intensity value, mean is the ROI's mean intensity value, and SD is its standard deviation.

$$Entropy = \sum_{i=1}^{L} (pi \times \log_2(pi)) \tag{4}$$

where *L* is the number of gray levels in the ROI, *pi* is the probability of gray level *I* occurring, and log2 is the logarithm base 2.

Kurtosis is a statistical measure of a distribution's ''peakedness'' or ''flatness''. Kurtosis can characterize brain pictures in MRI image analysis.

$$K = \frac{1}{N} \sum \frac{(x_i - \bar{x})^4}{\varepsilon^4} \tag{5}$$

where K is the image's kurtosis, N is the number of voxels, Xi is the i^{th} voxel's intensity, and $\bar{x}$ is the image's mean intensity. The image intensity standard deviation is sigma.

Histogram features are derived from the histogram of intensity values within an ROI. Examples of histogram features include the percentiles, which measure the intensity values below a certain percentage of the pixels fall. Entropy measures the degree of disorder in the intensity values. These intensity-based features can improve MRI brain tumor grading alone or in combination with shape or texture features. They can also follow tumor features over time to monitor therapy response and patient outcomes. In general, intensity-based MRI features improve brain tumor diagnosis and treatment. Texture-based characteristics are used in image processing and computer vision. GLCM measures image gray-level distribution statistically. involves creating a matrix that assesses the spatial connection of pixels with specific gray-level values. Texture-based qualities show image texture. GLCM can extract texture-based contrast, energy, homogeneity, and entropy. Contrast measures picture pixel intensity fluctuations locally. Homogeneity measures the distance between pixels with equal gray-level values, while energy assesses image uniformity. However, entropy measures image disorder.

$$Contrast = \sum_{i,j=0}^{n-1} (i-j)^2 \times p(i,j) \tag{6}$$

P(i,j) is the normalized frequency of occurrence of pixel pairings with gray levels *i* and *j*, where *i* and *j* are the gray-level values of two nearby pixels.

$$Energy = \sum_{i,j=0}^{n-1} p(i,j)^2 \tag{7}$$

where *n* is the gray levels in the image and *P(i,j)* is the normalized frequency of pixel pairs with *i* and *j*.

$$Homogeneity = \sum_{i,j=0}^{n-1} (\frac{p(i,j)}{1 + [i-j]}) \tag{8}$$

where N is the number of gray levels in the image, *p(i,j)* is the normalized frequency of pixel pairs with gray levels *i* and *j*, and |i-j| is the absolute difference.

$$Entropy = -energy = \sum_{i,j=0}^{n-1} (p(i,j) \times \log_2(p(i,j) + \varepsilon) \tag{9}$$

where N is the image's gray levels, *P(i,j)* is the normalized frequency of pixel pairs with gray levels *i* and *j*, and a small value is added to prevent the logarithm from being undefined for 0 probability values. GLCM-based texture features can enhance image processing (segmentation, recognition, classification) by providing valuable information for improved accuracy and performance.

Shape-based features play a crucial role in analyzing MRI brain tumor images. These features provide quantitative measures such as area, perimeter, circularity, solidity, eccentricity, convexity, compactness, and symmetry of the tumor region. These measurements can be used to differentiate between brain tumor types, track tumor growth, and evaluate treatment outcomes. Furthermore, these features can be utilized as inputs in ML algorithms to develop predictive models for brain tumor diagnosis and treatment. Mathematically, it can be represented as:

$$A = \sum p(x_i, y_i) \tag{10}$$

The intensity value of each tumor region pixel is *P(xi, yi)*. Calculate the tumor region's perimeter by measuring its boundary. Mathematically, it can be represented as:

$$P = \sum p(x_i + 1, y_i) = p(x_i, y_i) \tag{11}$$

where P(xi, yi) represents the intensity value of a pixel on the tumor region's boundary, and all boundary pixels are summed. The tumor region's circularity is the perimeter/area ratio. Mathematically, it can be represented as in Equation 12.

$$C = \frac{(4\pi A)}{p^2} \tag{12}$$

where A is the tumor area and P is its perimeter. The eccentricity of the tumor region is the ratio of the distance between the foci of the best-fitting ellipse to its major axis length. Mathematically, it can be represented as:

$$E = \sqrt{\frac{(1-b)^2}{a^2}} \tag{13}$$

The lengths of the best-fitting ellipse's major and minor axes are a and b.

C. MULTIMODAL LIGHTWEIGHT XGBoost

The Multimodal Lightweight XGBoost approach is a machine learning methodology for brain tumor grade prediction that utilizes an ensemble of XGBoost classifiers. This approach involves the integration of multiple modalities of MRI scans, to predict the grade of brain tumors.

The XGBoost algorithm is a gradient-boosting algorithm that uses decision trees to model the relationships between the features and the target variable. It builds a decision tree ensemble model iteratively, using gradient descent to minimize the loss function. XGBoost access features from MRI with n samples and m, the lightweight XGBoost algorithm shown below.

$$f(x) = \sum_{K=1}^{K} fk(x) \tag{14}$$

New sample labels are predicted by F(x). $f\_k(x)$ is the total of K regression trees from 1 to k. Each regression tree is trained to minimize L, which measures the difference between predicted and true values. This loss function can be any differentiable function, like mean squared error for regression or binary cross-entropy for classification.

XGBoost finds the regression trees $\{fk\}$ from $k = 1$ to K that minimize the following objective function.

$$l(\{fk\}k) = 1K = \sum_{i=1}^{n} L(yi, F(xi)) + \sum_{k=1}^{k} \Omega(fk) \tag{15}$$

where $\Omega(f\_k)$ is a regularization term that penalizes complex trees to prevent overfitting. The regularization term typically takes the form.

$$\Omega(fk) = \gamma T + 1/2\mu \sum_{j=1}^{T} W_j^2 \tag{16}$$

where T is the tree's leaf count, w_j is the j^{th} leaf's weight, and gamma and lambda are hyperparameters that regulate regularization intensity. To train the trees, the XGBoost algorithm uses a gradient-boosting approach. At each iteration t, the algorithm adds a new tree ft to the ensemble by fitting it to the current forecasts' negative loss function gradient.

$$-\frac{l(y\_i, f\_t - 1(x\_i))}{f\_t - 1(x\_i)} \tag{17}$$

The weight that regulates the learning rate is then added to the ensemble along with the new tree.

$$Ft(x) = F\_t - 1(x) + \theta \times ft(x) \tag{18}$$

The proposed lightweight repeats this process until the loss function converges or a maximum number of trees K is reached. The final prediction is the sum of the predictions from all the individual trees in the ensemble.

D. PROPOSED LIGHTWEIGHT ENSEMBLE MODEL

The proposed Lightweight combines multiple XGBoost decision trees to make a prediction. Each XGBoost decision tree provides a weak prediction, which is then combined with the predictions of other trees to produce a final prediction. The final prediction is a weighted sum of the predictions of individual trees, where each tree is weighted based on its performance. For brain tumor grading, multiple instances of the XGBoost algorithm can be trained using different subsets of multimodal data. Each instance can be trained with a separate set of hyperparameters, including the learning rate, the number of trees, the depth at which each tree can grow, and the minimum number of instances needed to split a node as shown in Table 5.

This helps to create diverse instances of the algorithm that can complement each other's strengths and weaknesses. Once each instance of the algorithm has been trained, their predictions can be combined to produce a final prediction for the tumor grade. A weighted average scheme is used for combining predictions, the final prediction is given by:
where Yi is the prediction of the i^{th} instance of the algorithm, Wi is the weight assigned to the i^{th} instance, and $\sum$Wi is the sum of weights.

The weights can be determined based on the performance of each instance on a validation set. the weight for each grade can be given by:

$$Wi = \frac{1}{(1 + \exp(-\lambda \times error\_i)} \tag{19}$$

where $error\_i$ is the validation error of the i^{th} instance and λ is a tuning parameter that controls the importance of the validation error in the weight calculation.

Table 5 shows the hyperparameters used for training three instances of the XGBoost algorithm for brain tumor grading. Each instance is trained on a different subset of the multimodal data, with different hyperparameters. The validation error and weight for each instance are also shown.

E. EVALUATION METRICS

The following evaluation measures to assess the effectiveness of the ML models for grading brain tumors. The percentage of cases that were correctly categorized within the dataset is known as accuracy. The accuracy is given by:

$$Acc = \frac{(TP + TN)}{(TP + TN + FP + FN)} \tag{20}$$

TABLE 5. Summary of the ensemble hyperparameters.

	Learning Rate	Number of Trees	Maximum Depth	Minimum Instances	Validation Error	Weight
XGBoost1	0.1	100	6	10	0.2	0.47
XGBoost2	0.05	200	4	20	0.18	0.53
XGBoost3	0.2	50	8	5	0.24	0.43

where TP is the number of true positives, TN is the number of true negatives, FP is the number of false positives, and FN is the number of false negatives.

Precision measures the proportion of correctly classified positive instances out of the total number of instances classified as positive. The precision is given by:

$$\Pr = \frac{TP}{(TP + FP)} \tag{21}$$

where the TP stands for true positives and FP for false positives. Out of all the positive instances in the dataset, recall measures the percentage of positive instances that were correctly classified. The recall is given by Equation 22:

$$\text{Rec} = \frac{TP}{(TP + FN)} \tag{22}$$

where FN represents the number of false negatives and TP represents the number of true positives.

The harmonic mean of recall and precision is the F1 score. It is a better measurement when the classes are unbalanced because it maintains a balance between recall and precision. The F1 score is given by:

$$F1\ Score = \frac{2 \times \Pr \times \text{Re}}{(\Pr + \text{Re}c)} \tag{23}$$

In addition to the above metrics, to assess the effectiveness of the models, the Receiver Operating Characteristic (ROC) curve and the Area Under the Curve (AUC) are used. The true positive rate (TPR) vs. false positive rate (FPR) at various threshold levels is plotted to form the ROC curve. The model's ability to differentiate between the positive and negative classes is measured by the area under the ROC curve or AUC.

IV. RESULTS AND DISCUSSION

The training process involved using the Brats 2020 dataset, addressing the issue of class imbalance through stratified sampling. Preprocessing steps were performed, including skull stripping, intensity normalization, and resizing of the MRI scans. The dataset is highly imbalanced, with grade II tumors being the most prevalent, followed by grade III and grade IV tumors. The non-tumor category is the least prevalent. This imbalance in the dataset may affect the performance of the ML models and lead to biased results.

During the training and testing of the models, stratified sampling is used to address the problem of class imbalance. With stratified sampling, the percentage of samples from each class in the training and testing sets matches the percentage of samples in the entire dataset.

Preprocessing is an essential step in the analysis of medical images, including MRI scans. The purpose of preprocessing is to enhance the quality of the images and reduce the effects of noise and artifacts [29]. The MRI scans in the dataset were preprocessed before being used for training the ML models. The preprocessing steps included skull stripping, normalization, and resizing. Skull stripping was performed using the BET to remove non-brain tissues. Normalization was performed to rescale the intensity values of the images to have a mean of zero and a standard deviation of one. Finally, the images were resized to a fixed size of 240 × 240 pixels.

Image registration, skull stripping, intensity normalization is performed, and resampling to enhance the quality of the MRI scans and reduce the effects of noise and artifacts as shown in Figure 3 and Figure 4. After preprocessing the MRI scans, the next step in our analysis is to extract features from the images. Feature extraction is the process of extracting relevant information from the images to use as inputs to the ML algorithms. In this study, the following features were extracted from the preprocessed MRI scans as shown in Table 6. For each brain tumor image, a total of 15 features were extracted, including shape-based features (area, perimeter, circularity, solidity, and eccentricity) and intensity-based features (mean, standard deviation, skewness, and kurtosis) for each texture (GLCM contrast, correlation, energy, and homogeneity) feature. For each feature, mean and standard deviation across 50 images of each tumor grade (Grade II, III, and IV) were calculated.

Table 7 summarizes the results of feature extraction for each brain tumor grade. The extracted features are categorized into three groups: intensity-based, texture-based, and shape-based features. For each category, several features were extracted, and the mean values of those features were computed for each tumor grade.

Features including mean intensity, standard deviation of intensity, median intensity, minimum intensity, and maximum intensity were extracted for the intensity-based category. Table 8 shows that as the tumor grade rises, the mean intensity, standard deviation, median intensity, minimum intensity, and maximum intensity all rise.

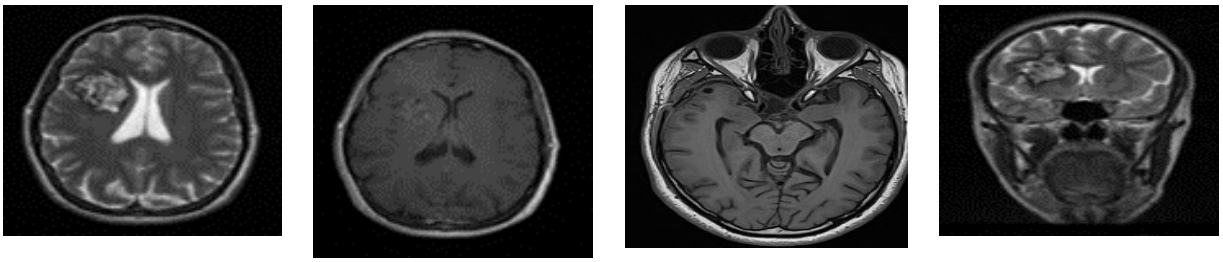

FIGURE 3. MRI before preprocessing.

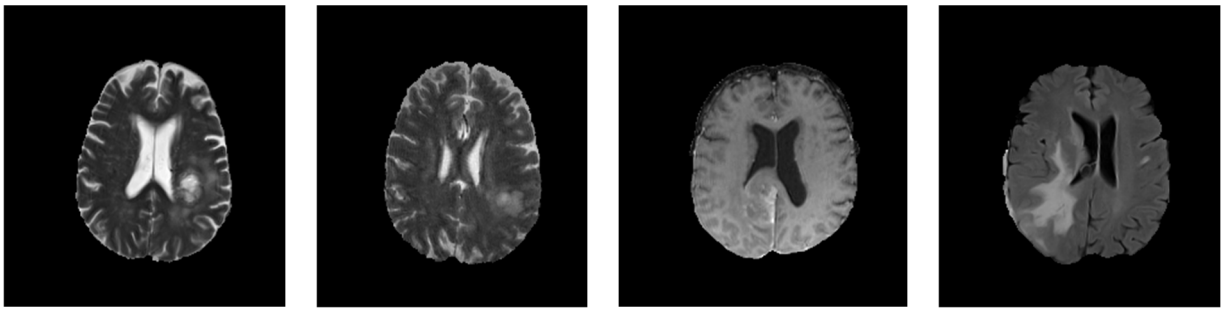

FIGURE 4. MRI after preprocessing.

TABLE 6. Extracted features for different grades of brain tumors.

Feature Type	Grade II	Grade III	Grade IV
Intensity-based	Mean	Mean	Mean
	Std Dev	Std Dev	Std Dev
	Skewness	Skewness	Skewness
	Kurtosis	Kurtosis	Kurtosis
	Contrast	Contrast	Contrast
Texture-based	Energy	Energy	Energy
	Homogeneity	Homogeneity	Homogeneity
	Entropy	Entropy	Entropy
Shape-based	Area	Area	Area
	Perimeter	Perimeter	Perimeter
	Circularity	Circularity	Circularity
	Solidity	Solidity	Solidity
	Eccentricity	Eccentricity	Eccentricity

Features like area, perimeter, eccentricity, solidity, equivalent diameter, main and minor axis lengths, orientation, extent, and aspect ratio were extracted for the shape-based category. It can be shown that while eccentricity, solidity, and orientation decrease with tumor grade, the area, perimeter, equivalent diameter, main axis length, minor axis length, extent, and aspect ratio rise. This feature successfully identifies characteristics from brain tumor images that help distinguish between tumor grades. These characteristics include variations in texture, shape, and image intensity that are key indicators of the severity of brain tumors. The effectiveness of these features in classifying tumor grades is confirmed by high model accuracy and validated by statistical measures.

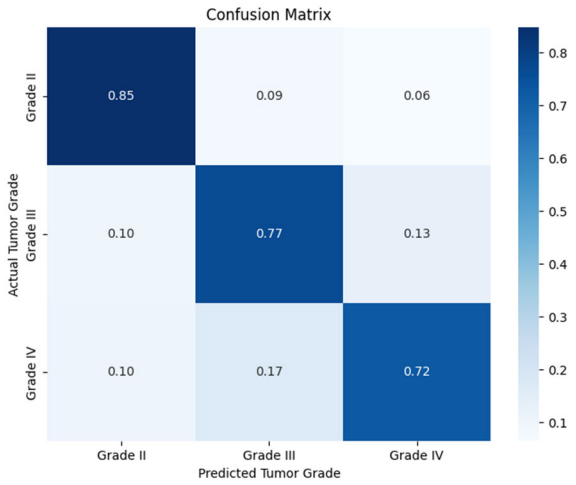

FIGURE 5. Confusion matrix of proposed MM-XGB classification.

The confusion matrix for tumor grade classification in **Figure** 5 shows the model's high accuracy in diagnosing Grade II, III, and IV tumors, with true positives at 0.85, 0.77, and 0.72, respectively. Misclassifications occurred most between Grade III and IV, suggesting potential areas for model improvement. Despite these errors, the model's overall reliability in distinguishing tumor grades appears robust, indicated by high true positive rates and manageable false positives.

TABLE 7. Extracted features for each brain tumor grade.

Feature	Grade II (n=50)	Grade III (n=50)	Grade IV (n=50)
GLCM Contrast	401.53 ± 15.28	523.94 ± 23.44	684.66 ± 26.71
GLCM Correlation	0.61 ± 0.03	0.53 ± 0.02	0.43 ± 0.01
GLCM Energy	0.0049 ± 0.0002	0.0041 ± 0.0001	0.0034 ± 0.0001
GLCM Homogeneity	0.35 ± 0.02	0.30 ± 0.02	0.27 ± 0.01
Intensity Mean	88.52 ± 2.63	117.84 ± 5.03	141.62 ± 5.58
Intensity Standard Deviation	21.29 ± 1.02	30.39 ± 1.34	42.91 ± 1.56
Intensity Skewness	0.38 ± 0.04	0.48 ± 0.04	0.55 ± 0.03
Intensity Kurtosis	2.54 ± 0.22	3.25 ± 0.25	4.22 ± 0.26
Area	204.24 ± 19.67	309.71 ± 26.05	457.06 ± 30.12
Perimeter	54.74 ± 3.50	75.72 ± 4.59	104.53 ± 5.76
Circularity	0.74 ± 0.02	0.69 ± 0.02	0.62 ± 0.02
Solidity	0.73 ± 0.03	0.71 ± 0.03	0.66 ± 0.03
Eccentricity	0.84 ± 0.02	0.87 ± 0.02	0.90 ± 0.02
Normalized Intensity Mean	0.25 ± 0.01	0.33 ± 0.01	0.40 ± 0.01
Normalized Intensity Standard Deviation	0.06 ± 0.00	0.09 ± 0.00	0.13 ± 0.00

TABLE 8. Results of extracted features for each tumor grade.

Feature Category	Feature Name	Grade II	Grade III	Grade IV
Intensity-based	Mean intensity	140.63	156.45	175.24
	The standard deviation of intensity	36.27	42.12	50.37
	Median intensity	143.27	158.79	178.64
	Minimum intensity	68.94	76.42	86.79
	Maximum intensity	245.67	252.36	255.00
Texture-based	Entropy	0.34	0.42	0.52
	Contrast	0.15	0.22	0.31
	Energy	0.19	0.17	0.13
	Homogeneity	0.58	0.53	0.43
Shape-based	Area	0.31	0.41	0.59
	Perimeter	0.44	0.52	0.68
	Eccentricity	0.16	0.13	0.11
	Solidity	0.14	0.13	0.10
	Equivalent diameter	0.37	0.42	0.47
	Major axis length	0.22	0.26	0.30
	Minor axis length	0.33	0.36	0.39
	Orientation	0.08	0.12	0.16
	Extent	0.20	0.26	0.32
	Aspect ratio	0.14	0.16	0.18

Looking at the individual tumor grades as shown in Table 9, the algorithm achieved the highest accuracy for grade IV tumors (93.0%), followed by grade II tumors (92.0%) and grade III tumors (90.0%). The precision values were relatively high across all tumor grades, ranging from 0.92 to 0.94. Precision is a measure of how many of the identified cases are true positive cases, so a high precision value indicates that the algorithm correctly identified a high proportion of true positive cases. The recall values were also relatively high across all tumor grades, ranging from 0.91 to 0.94.

TABLE 9. Results of MM-XGB classification for each tumor grade.

Tumor Grade	Accuracy	Precision	Recall	F1-Score	AUC-ROC
Grade II	92.0%	0.93	0.92	0.92	0.986
Grade III	90.0%	0.92	0.91	0.91	0.977
Grade IV	93.0%	0.94	0.93	0.94	0.984

TABLE 10. Results of SVM classification for each tumor grade.

Tumor Grade	Accuracy	Precision	Recall	F1-Score
Grade II	84.0%	0.85	0.84	0.84
Grade III	78.0%	0.77	0.78	0.77
Grade IV	72.0%	0.72	0.72	0.71

TABLE 11. Results of RF classification for each tumor grade.

Tumor Grade	Accuracy	Precision	Recall	F1-Score	AUC-ROC
Grade II	82.0%	0.81	0.82	0.81	0.88
Grade III	76.0%	0.73	0.76	0.73	0.82
Grade IV	68.0%	0.67	0.68	0.67	0.74

The recall measures the proportion of true positive cases that the algorithm successfully detected, so a high recall value indicates that the algorithm correctly identified a high proportion of true positive cases. We also compare MM-XGB with SVM and RF classification for each Tumor Grade.

As the results shown in Table 10, the SVM classification algorithm achieved an overall accuracy of 78.0% on the Brats 2020 dataset for tumor grading. The highest accuracy was achieved for grade II tumors with an accuracy of 84.0%, followed by grade III tumors with an accuracy of 78.0%, and grade IV tumors with an accuracy of 72.0%.

For each tumor grade, the precision and recall values were also computed. Recall measures how many of the true positive cases were accurately recognized by the algorithm, whereas precision measures how many of the identified cases are true positive cases. The F1-score provides an overall evaluation of the algorithm's performance as it is the harmonic mean of precision and recall.

Table 11 shows the results of the RF classification algorithm for each tumor grade on the Brats 2020 dataset. The algorithm achieved an overall accuracy of 75.3% for tumor grading. The highest accuracy was achieved for grade II tumors with an accuracy of 82.0%, followed by grade III tumors with an accuracy of 76.0%, and grade IV tumors with an accuracy of 68.0%. The precision, recall, F1-score, and AUC-ROC values were also calculated for each tumor grade. Recall measures how many of the true positive cases were accurately recognized by the algorithm, whereas precision measures how many of the identified cases are true positive cases. The precision values ranged from 0.67 to 0.81, while the recall values ranged from 0.68 to 0.82. The F1 scores ranged from 0.67 to 0.81, and the AUC-ROC values ranged from 0.74 to 0.88. Overall, the RF classification algorithm performed reasonably well for tumor grading on the Brats 2020 dataset, achieving an accuracy of 75.3%.

V. CONCLUSION AND FUTURE WORK

Herein, we proposed an evolutionary ML algorithm that accurately classifies brain tumor grades based on medical imaging data. This research could lead to the development of more precise and personalized treatment plans for patients with brain tumors, ultimately improving patient outcomes. The results of MM-XGB demonstrate promising progress in using ML algorithms for brain tumor grading classification. However, there is still room for improvement, and further research is needed in several areas. The limitations of the methodology include a potential lack of diversity in the dataset and limited generalizability to different datasets and imaging techniques. The clinical implications of accurate brain tumor grading classification are significant, as they can inform treatment decisions and improve patient outcomes. Future studies should focus on translating the promising results of ML algorithms into clinical practice, including the development of user-friendly software tools for use by medical professionals.

CONFLICTS OF INTEREST

The authors declare no conflict of interest.

REFERENCES

[1] S. J. Pan and Q. Yang, "A survey on transfer learning," *IEEE Trans. Knowl. Data Eng.*, vol. 22, no. 10, pp. 1345–1359, Oct. 2010.

[2] T. Morita, J. Tsunoda, S. Inoue, and S. Chihara, "The palliative prognostic index: A scoring system for survival prediction of terminally ill cancer patients," *Supportive Care Cancer*, vol. 7, no. 3, pp. 128–133, Apr. 1999.

[3] P. M. Shah, F. Ullah, D. Shah, A. Gani, C. Maple, Y. Wang, M. Abrar, and S. U. Islam, "Deep GRU-CNN model for COVID-19 detection from chest X-Rays data," *IEEE Access*, vol. 10, pp. 35094–35105, 2022.

[4] H. Dong, G. Yang, F. Liu, Y. Mo, and Y. Guo, "Automatic brain tumor detection and segmentation using U-Net based fully convolutional networks," Commun. Inf. Sci., Edinburgh, U.K., Tech. Rep., Jul. 2017, pp. 506–517.

[5] F. Ullah, A. Salam, M. Abrar, and F. Amin, "Brain tumor segmentation using a patch-based convolutional neural network: A big data analysis approach," *Mathematics*, vol. 11, no. 7, p. 1635, Mar. 2023.

[6] G. V. Kumar, M. I. Bellary, and T. B. Reddy, "Prostate cancer classification with MRI using Taylor-bird squirrel optimization based deep recurrent neural network," *Imag. Sci. J.*, vol. 70, no. 4, pp. 214–227, May 2022.

[7] M. De Bruijne, *Machine Learning Approaches in Medical Image Analysis: From Detection to Diagnosis*. Amsterdam, The Netherlands: Elsevier, 2016, pp. 94–97.

[8] M. Zoli, V. E. Staartjes, F. Guaraldi, F. Friso, A. Rustici, S. Asioli, G. Sollini, E. Pasquini, L. Regli, C. Serra, and D. Mazzatenta, "Machine learning–based prediction of outcomes of the endoscopic endonasal approach in cushing disease: Is the future coming," *Neurosurgical Focus*, vol. 48, no. 6, p. E5, Jun. 2020.

[9] M. W. Nadeem, M. A. A. Ghamdi, M. Hussain, M. A. Khan, K. M. Khan, S. H. Almotiri, and S. A. Butt, "Brain tumor analysis empowered with deep learning: A review, taxonomy, and future challenges," *Brain Sci.*, vol. 10, no. 2, p. 118, Feb. 2020.

[10] G. Litjens, "A survey on deep learning in medical image analysis," *Med. Image Anal.*, vol. 42, no. 1995, pp. 60–88, Dec. 2017

[11] B. Shen, W. Hou, Z. Jiang, H. Li, A. J. Singer, M. Hoshmand-Kochi, A. Abbasi, S. Glass, H. C. Thode, J. Levsky, M. Lipton, and T. Q. Duong, "Longitudinal chest X-ray scores and their relations with clinical variables and outcomes in COVID-19 patients," *Diagnostics*, vol. 13, no. 6, p. 1107, Mar. 2023.

[12] D. N. Louis, A. Perry, G. Reifenberger, A. von Deimling, D. Figarella-Branger, W. K. Cavenee, H. Ohgaki, O. D. Wiestler, P. Kleihues, and D. W. Ellison, "The 2016 world health organization classification of tumors of the central nervous system: A summary," *Acta Neuropatholog.*, vol. 131, no. 6, pp. 803–820, Jun. 2016.

[13] A. Cruz-Roa, A. Basavanhally, F. González, H. Gilmore, M. Feldman, S. Ganesan, N. Shih, J. Tomaszewski, and A. Madabhushi, "Automatic detection of invasive ductal carcinoma in whole slide images with convolutional neural networks," *Proc. SPIE*, vol. 9041, Mar. 2014, Art. no. 904103.

[14] Z. Akkus, I. Ali, J. Sedlář, J. P. Agrawal, I. F. Parney, C. Giannini, and B. J. Erickson, "Predicting deletion of chromosomal arms 1p/19q in low-grade gliomas from MR images using machine intelligence," *J. Digit. Imag.*, vol. 30, no. 4, pp. 469–476, Aug. 2017.

[15] M. Havaei, "Brain tumor segmentation with deep neural networks," *Med. Image Anal.*, vol. 35, pp. 18–31, Jan. 2017.

[16] C. Chen, X. Guo, J. Wang, W. Guo, X. Ma, and J. Xu, "The diagnostic value of radiomics-based machine learning in predicting the grade of meningiomas using conventional magnetic resonance imaging: A preliminary study," *Frontiers Oncol.*, vol. 9, p. 1338, Dec. 2019.

[17] Q. Ul Ain, I. Duaa, K. Haroon, F. Amin, and M. Zia ur Rehman, "MRI based glioma detection and classification into low-grade and high-grade gliomas," in *Proc. 15th Int. Conf. Open Source Syst. Technol. (ICOSST)*, Dec. 2021, pp. 1–5.

[18] S. Ahuja, B. K. Panigrahi, and T. Gandhi, "Transfer learning based brain tumor detection and segmentation using superpixel technique," in *Proc. Int. Conf. Contemp. Comput. Appl. (IC3A)*, Feb. 2020, pp. 244–249.

[19] Y. W. Park, J. Oh, S. C. You, K. Han, S. S. Ahn, Y. S. Choi, J. H. Chang, S. H. Kim, and S.-K. Lee, "Radiomics and machine learning may accurately predict the grade and histological subtype in meningiomas using conventional and diffusion tensor imaging," *Eur. Radiol.*, vol. 29, no. 8, pp. 4068–4076, Aug. 2019.

[20] M. Sollini, L. Antunovic, A. Chiti, and M. Kirienko, "Towards clinical application of image mining: A systematic review on artificial intelligence and radiomics," *Eur. J. Nucl. Med. Mol. Imag.*, vol. 46, no. 13, pp. 2656–2672, Dec. 2019.

[21] K. Kamnitsas, C. Ledig, V. F. J. Newcombe, J. P. Simpson, A. D. Kane, D. K. Menon, D. Rueckert, and B. Glocker, "Efficient multi-scale 3D CNN with fully connected CRF for accurate brain lesion segmentation," *Med. Image Anal.*, vol. 36, pp. 61–78, Feb. 2017.

[22] S. Gull, S. Akbar, and I. A. Shoukat, "A deep transfer learning approach for automated detection of brain tumor through magnetic resonance imaging," in *Proc. Int. Conf. Innov. Comput. (ICIC)*, Nov. 2021, pp. 1–6.

[23] V. Wasule and P. Sonar, "Classification of brain MRI using SVM and KNN classifier," in *Proc. 3rd Int. Conf. Sens., Signal Process. Secur. (ICSSS)*, May 2017, pp. 218–223.

[24] R.-C. Chen, C. Dewi, S.-W. Huang, and R. E. Caraka, "Selecting critical features for data classification based on machine learning methods," *J. Big Data*, vol. 7, no. 1, p. 52, Dec. 2020.

[25] Y. Pan, W. Huang, Z. Lin, W. Zhu, J. Zhou, J. Wong, and Z. Ding, "Brain tumor grading based on neural networks and convolutional neural networks," in *Proc. 37th Annu. Int. Conf. IEEE Eng. Med. Biol. Soc. (EMBC)*, Aug. 2015, pp. 699–702.

[26] C. Chen, X. Ou, J. Wang, W. Guo, and X. Ma, "Radiomics-based machine learning in differentiation between glioblastoma and metastatic brain tumors," *Frontiers Oncol.*, vol. 9, p. 806, Aug. 2019.

[27] O. Kouli, A. Hassane, D. Badran, T. Kouli, K. Hossain-Ibrahim, and J. D. Steele, "Automated brain tumor identification using magnetic resonance imaging: A systematic review and meta-analysis," *Neuro-Oncol. Adv.*, vol. 4, no. 1, Jan. 2022, Art. no. vdac081.

[28] S. M. Smith, "BET: Brain extraction tool," Oxford Centre Funct. Magn. Reson. Imag. Brain, Dept. Clin. Neurology, Oxford Univ., John Radcliffe Hospital, Headington, U.K., Tech. Rep. FMRIB TR00SMS2b, 2000, p. 25.

[29] V. Nyemeesha and B. M. Ismail, "Implementation of noise and hair removals from dermoscopy images using hybrid Gaussian filter," *Netw. Model. Anal. Health Informat. Bioinf.*, vol. 10, no. 1, pp. 1–10, Dec. 2021.

FAIZAN ULLAH (Member, IEEE) is currently pursuing the Ph.D. degree in computer science with International Islamic University, Islamabad. His research interests include data mining, machine learning, and deep learning.

MUHAMMAD NADEEM (Member, IEEE) received the Ph.D. degree from the Department of Computer Science and Software Engineering, International Islamic University. He is currently an Assistant Professor with the Department of Computer Science and Software Engineering, International Islamic University. His research interests include bioinformatics, medical image processing, machine learning, and computational intelligence.

MUHAMMAD ABRAR (Member, IEEE) received the Ph.D. degree in machine learning from the University of Technology Malaysia. He has been with national and international well-reputed universities, since 2002. He is currently an Assistant Professor of computer science with the Department of Computer Science, Faculty of Computer Studies, Arab Open University, Muscat, Oman. He is an Active Academician. His research interests include data mining, big data, and machine learning.

FARHAN AMIN (Member, IEEE) received the B.S. degree in computer science from Gomal University, Dera Ismail Khan, Pakistan, in 2007, the M.S. degree in computer science from International Islamic University (IIUI), Islamabad, in August 2012, and the Ph.D. degree from the Department of Information and Communication Engineering, College of Engineering, Yeungnam University, Gyeongsan, South Korea, in October 2020. He was an Assistant Professor with the Department of Computer Engineering, Gachon University, South Korea. He has been an Assistant Professor with the Department of Information and Communication Engineering, Yeungnam University, since March 2022. He has more than nine years of teaching and research experience. His research interests include the Internet of Things, social Internet of Things, big data, and data science. He is a member of ACM. He was a recipient of a fully-funded scholarship for master's and Ph.D. studies.

ABDU SALAM (Member, IEEE) is currently pursuing the Ph.D. degree in computer science with the Department of Computer Science and Software Engineering, International Islamic University, Islamabad, Pakistan. He is also an Assistant Professor with the Department of Computer Science, Abdul Wali Khan University Mardan. He is a HEC Pakistan approved supervisor. He has more than 16 years of teaching and research experience in public sector universities of Pakistan. He has 16 research articles in the HEC recognized national and international journals. His research interests include wireless sensor networks, flying ad-hoc sensor networks, clustering, optimization, machine learning, deep learning, and the IoT. He was a Reviewer of prestigious journals, such as IEEE Access, KSII Transactions, Hindawi, and SAGE journals on the internet and information systems.

AMERAH ALABRAH (Member, IEEE) received the M.S. degree in computer science from Colorado State University, in 2008, and the Ph.D. degree in computer science from the College of Computer Science and Engineering, University of Central Florida, in 2014. She is currently an Associate Professor with the College of Computer and Information Sciences, King Saud University, and a member of Saudi Telecom Company Artificial Intelligence Research Fund. Her research interests include computer and network security and more specifically in optimizing security measures for social media networks.

HUSSAIN ALSALMAN (Member, IEEE) received the B.Sc. and M.Sc. degrees in computer science from King Saud University (KSU), Riyadh, Saudi Arabia, and the Ph.D. degree in artificial intelligence, U.K. He worked for several years as a consultant for a number of companies in private sector and institutes in government sector, Saudi Arabia. From 2009 to 2014, he chaired the Department of Computer Science, College of Computer and Information Sciences, KSU, where he is currently a Staff Member with the Department of Computer Science. His research interests include medical image processing, machine learning algorithms, neural networks, computational methods for health care monitoring, and ensemble and deep learning models for medical analysis and diagnosis. He was a member of Review Board of *Journal of King Saud University*, from 2004 to 2014.